University of Wollongong
Research Online

Faculty of Engineering - Papers (Archive)

Faculty of Engineering and Information Sciences

2001

Design and simulation of continuous scintillator with pixellated photodetector

G. J. Takacs
University of Wollongong, gjt@uow.edu.au

Anatoly B. Rosenfeld
University of Wollongong, anatoly_rozenfeld@uow.edu.au

M. L. Lerch
University of Wollongong, mlerch@uow.edu.au

Publication Details

This article was originally published as: Takacs, G, Rosenfeld, A & Lerch, MLF, Design and Simulation of Continuous Scintillator with Pixellated Photodetector, IEEE Transactions on Nuclear Science, August 2001, 48(4)2, 1412-1417. Copyright IEEE 2001.

Research Online is the open access institutional repository for the University of Wollongong. For further information contact the UOW Library: research-pubs@uow.edu.au

Design and Simulation of Continuous Scintillator With Pixellated Photodetector

George J. Takacs, *Member, IEEE*, Anatoly B. Rosenfeld, *Senior Member, IEEE*, and Michael L. F. Lerch, *Member, IEEE*

***Abstract*—We present results of simulations performed as part of the development of a gamma-ray detector module comprising a nonpixellated scintillator and pixellated photodiode detector. The simulations have been carried out to determine the effect of surface treatment and dimensions of the scintillator on the ability to determine the two-dimensional position of interaction. A set of 32 different combinations of surface treatments have been considered for each crystal size. Scintillator dimensions considered have been 25 × 25 × (3–6 mm^3). For scintillator thicknesses at the low end of this range, an average accuracy of 0.5–0.6 mm is achievable for many different surface treatments. At the higher end of the thickness range, 6 mm, the average accuracy reduces to around 0.7 mm and is more dependent on the surface treatment.**

***Index Terms*—Light propagation, Monte Carlo simulation, positron emission tomography (PET), scintillators.**

I. Introduction

DURING the last decade, the combination of scintillator-silicon photodetectors (PDs) are finding increasing applications in nuclear medicine instrumentation, particularly in mammography [1] and positron emission tomography (PET) detector modules [2]. Such applications have been made possible due to essential improvements in PD quality (low noise, improved spectral sensitivity between the wavelength region 420–600 nm), development of multichannel readout CMOS single chips [3],[4], and availability of pixellated scintillators [1]. However, pixellated scintillators in conjunction with silicon pixel PDs demand light isolation between each pixel, which reduces the efficiency of the detector due to the reduction in size of the scintillator pixel. The aim of present development is to investigate the possibility of three-dimensional (3-D) detection of position of interaction (POI) of the gamma photon in a nonpixellated scintillator crystal optically attached to silicon pixel PD array. Such detectors could then be used as the basis of SPECT and PET detector modules that are independent of photomultiplier tubes.

The silicon arrays to be used consist of 64 photodiodes, each 3 mm by 3 mm, in a square array 25 mm long. These are to be coupled, using optical grease, to one face of a scintillator crystal, of area 25 × 25 mm^2, with thicknesses from 3 to 6 mm. The remaining surfaces of the scintillator crystal may be covered with diffuse or specular reflectors. The modules as described could then be used edge-on, with most of the gamma rays entering through a 25 × 3 mm^2 face, or front-on with the gamma-rays entering primarily through the face opposite the diode array. Two materials have been considered for the scintillator: CsI(Tl) or LSO. These are very different in terms of their light output (both spectral content and amount), attenuation coefficient, and decay times but have very similar refractive indexes. These parameters are summarized inTable I[5], [6].

TABLE I
SCINTILLATOR PROPERTIES

Property	LSO	CsI(Tl)
Refractive Index	1.82	1.79
Attenuation for 511keV	0.88 cm^{-1}	0.45 cm^{-1}
e-h pairs for 511 keV	9 300	20 000

For the proposed detector modules, it is important that the dimensions and surface treatment of the scintillator crystals are chosen to maximize the resolution of the detector. The detector resolution is determined by the ability to calculate, from the signals of the photodiode array, the coordinates of the point of interaction of the γ-ray in the crystal. Thus it is desirable to have a simulation code that 1) enables the study of the light propagation in the scintillator and how the detected light is distributed between the pixels of the photodiode array and 2) uses this light distribution to calculate the point of interaction of the gamma-ray in the scintillator. In the past, many people have used Monte Carlo codes to study the propagation of light in scintillator crystals. However, due to our quite specific requirements, it was decided to develop our own code. The simulations performed for this paper are similar in one respect to those of Siegel *et al.* [6], using the DETECT [7] program, in that we create a pixel image of the light distribution on the photodetector surface. However, we do so here for the specific purpose of calculating the two-dimensional (2-D) interaction position and determining how the accuracy of this calculation varies with surface treatment.

II. Description of Detector Module

The 25 × 25 mm^2 silicon 8 × 8 PD was developed in collaboration with SPA "Detector."[1] Each 3 × 3 mm^2 PD has low noise level (reverse current of 0.1 nA at full depletion) and energy resolution for 662-keV gamma photons of 8% with CsI(Tl) and 23% with LSO [8].

In contrast to other developments [9], our design of n-Si pixel PD allows for the attachment of a 25 × 25 mm^2 scintillator

Manuscript received November 2, 2000; revised May 16, 2001. This work was supported by the Department of Industry, Science and Resources, Australia, and by the National Health and Medical Research Council, Australia, under Grant 980493.

The authors are with the Centre for Medical Radiation Physics, Faculty of Engineering, University of Wollongong, 2522 N.S.W., Australia (e-mail: george_takacs@uow.edu.au).

Publisher Item Identifier S 0018-9499(01)07402-0.

[1]Scientific Production Association, Kiev, Ukraine.

0018–9499/01$10.00 ©2001 IEEE

crystal on the p^+ side of the PD. The aim of this design is to enhance the time properties of the detector module in coincidence mode, due to the fast hole collection near the surface of the p^+ region.

For imaging applications, the parallel readout of all pixels is required. The signal output pads of the pixel PD have a 90μm pitch and are all located on one side of PD, allowing easy connection to a VIKING readout chip. VIKING is a high-speed 128-channel chip designed for strip detectors used in high-energy physics (HEP) applications and is well known [4]. The low rms noise of about 150 electrons for several picofarads input capacitance of each pixel, and low cost, together with its proven ability in the application of data acquisition used in HEP vertex detectors, make this chip attractive for medical imaging instrumentation. The limitation of the PD pixel size in such design is due to the signal-to-noise ratio, which depends not just on the pixel capacitance and reverse bias leakage current but also on the number of photons reaching the pixel element and noise of electronics.

III. Simulations of Light Distribution

A. Description of the Simulation Code

The simulation code we have developed has two main functions. The first is to simulate the transport of scintillation light photons in the scintillator and the second is to calculate the interaction position.

To simulate the propagation of scintillation light in the crystal, we generate a specified number of photons, at a point in the crystal, with randomly chosen directions with uniform probability per unit solid angle. The point of intersection of the photon trajectory and the scintillator surface is determined and the surface conditions are then used along with the Fresnel relations for unpolarized light to determine the reflection probability and scattered direction. We have not considered scattering or attenuation of light within the crystal volume, due to the small average path lengths of the scintillation photons.

Surfaces are treated as either rough or smooth. The treatment of reflection used in the code essentially follows that used by Bea *et al.*, [10] and is similar to that in DETECT97 [7], [11]. Rough surfaces are described using a facet model, with a Gaussian distribution of slopes of standard deviation equal to the rms slope. This is slightly different from the model in DETECT97, where the angles of the facets are assumed to follow a Gaussian distribution. However, for small rms slopes, the models will be equivalent. Another difference from the DETECT97 is that we have not implemented any of the spike or lobe constants described as part of the UNIFIED model of reference [11].

Surfaces may be specified as being clad with a diffuse reflective material, specular reflector, detectors, or uncovered. For diffuse reflection, we have assumed Lambert's law so that the probability for reflection at an angle θ to the surface normal is independent of incident angle and proportional to $\sin 2\theta d\theta$. A small air gap is assumed to exist between the scintillator and any cladding material.

Each photon is followed until it exits the scintillator plus any cladding. If a photon exits on the photodetector surface, the count for the diode it enters is incremented. After the selected number of photons have left the scintillator, the code calculates the x and y coordinates of the point of the γ-ray interaction using the number of photons incident on the photodiodes plus any noise.

Photodiode noise and its effects are simulated by adding to the counts for each photodiode a random number of counts, specified by an rms value, varying between rms/2 and $3 \times \text{rms}/2$ with a triangular distribution. We have assumed a noise figure of 200 rms.

Various algorithms have been trialed for calculating the POI. These include:

1) polynomial fits to the diode counts along two orthogonal lines of diodes through the maximum position;
2) modified Anger logic;
3) using the highest diode and all neighboring diodes;
4) linear combinations of the coordinates of the diode center for the n highest diodes.

In this latter case, we also tried weighting the diode coordinates both proportionally to the number of photons incident on each diode and proportionally to the square of the number incident on the diode. Of the four approaches, the final method is consistently and significantly better than the others, and all POI results presented in this paper are for the final method. While a full discussion of the results from these algorithms is outside the scope of this paper, it is worth noting that when the scintillator surfaces are rough, the quadratic weighting of diode coordinates gives a significantly better result than a first-order weighting. If all surfaces are smooth, however, then the two weighting schemes give about the same result (in terms of the magnitude of the error in POI). We have also found that the best results are obtained when $n = 4$, that is, only the four highest diode counts are used.

Output from the code consists of:

1) the coordinates of each scintillator photon incident on the photodiode array;
2) the number of photons incident on each photodiode;
3) the x and y coordinates of the interaction point;
4) the calculated x and y coordinates of the interaction point using various algorithms;
5) the error between the calculated and actual gamma-ray position of interaction in the xy plane for the respective algorithm.

An example showing the number of photons incident on each diode in an 8×8 photodiode detector array is given in Fig. 1. The crystal surfaces are unclad and smooth and the total number of scintillator photons generated was 25 000. The noteworthy feature from this figure is that about 60% of detected photons are in four bins.

The simulations reported here have been carried out using a refractive index of 1.8 for the scintillator. This value is close to that for both CsI and LSO. Outside all surfaces, except the photodetector surface, the refractive index has been taken as 1.0, while on the photodetector surface, a value of 1.5 has been assumed. We make the assumption that any photon exiting through

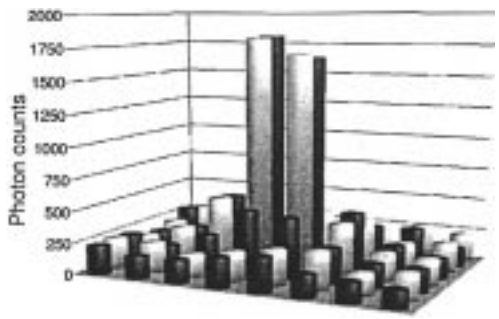

Fig. 1. Distribution of detected photons plus noise for interaction point in the center of the scintillator.

the photodetector surface is absorbed in the detector. For all the simulations reported here, unless stated otherwise, 25 000 photons have been generated at each gamma-ray interaction point. This value is about the number to be expected for 511-keV gammas incident on CsI scintillators. When cladding has been specified, it has been assumed to have a reflectivity of 0.95.

B. Surface Treatment Effects

To examine the effect of surface treatment on the accuracy of determination of the 2-D POI, the simulation code was used as follows for each set of surface conditions. First, a point is generated at random within the volume of the crystal. After the specified number of photon histories, noise is added to each diode count, and the diode counts are used to calculate the 2-D POI and the magnitude of the difference between the real 2-D POI and the calculated 2-D POI (the error). This process is carried out for 1000 randomly chosen interaction points, and the average error is then calculated. This process is repeated for a total of 32 combinations of surface treatments.

The results of this are summarized in Table II for crystals of dimensions $25 \times 25 \times 3\,\mathrm{mm}^3$ and $25 \times 25 \times 6\,\mathrm{mm}^3$. In this table, "top" refers to the photodetector surface, "s"means that the surface was smooth, "r" means that the surface was rough, "u" means uncovered, and "c" means clad with a diffuse reflector. All rough surfaces in this table were modeled as having facets with slopes of standard deviation equal to one, which is quite rough. The column labeled "output" gives the percent of generated photons that exit the top (detector) surface. The error is the average error over the 1000 points randomly selected within the crystal and is in millimeters. In all cases, it has been calculated using a weighted average of the coordinates of the four highest diodes. By repeating these simulations with different seeds for the random number generator, we have determined the 95% confidence level in 2-D POI errors to be 0.02 mm and 0.1% for the light output. The letter "l" next to the error indicates a first order weighting, while "q" denotes a second-order or quadratic weighting.

From these results, it is quite clear that for the 3-mm-thick crystal, the surface treatment has only a small effect on the accuracy. This is despite there being quite a large variation in the light output for different surface treatments. However, for the 6-mm-thick crystal, there is a pronounced variation. For both thicknesses, whether the photodetector surface is rough or smooth seems to have little effect. When we compare the results

TABLE II
DEPENDENCE OF 2-D POI ACCURACY ON SURFACE TREATMENT, WITH 25 000 PHOTONS PER INTERACTION AND 200 E^- rms PER DIODE

Surface					Thickness 3 mm		Thickness 6 mm	
Sides		Bottom		Top	Output	Error	Output	Error
s	u	s	u	s	37.3	0.64 (l)	37.3	0.86 (q)
s	u	s	u	r	54.4	0.61 (l)	49.3	0.79 (q)
s	u	s	c	s	44.2	0.52 (l)	44.2	0.66 (q)
s	u	s	c	r	61.2	0.53 (l)	56.0	0.59 (q)
s	u	r	u	s	51.6	0.61 (l)	46.7	0.75 (q)
s	u	r	u	r	52.1	0.57 (l)	45.4	0.72 (q)
s	u	r	c	s	61.9	0.56 (l)	56.3	0.72 (q)
s	u	r	c	r	61.2	0.55 (l)	53.6	0.65 (q)
s	c	s	u	s	37.3	0.62 (q)	37.3	0.90 (q)
s	c	s	u	r	86.5	0.63 (q)	75.3	0.85 (q)
s	c	s	c	s	44.2	0.55 (l)	44.2	0.72 (q)
s	c	s	c	r	94.4	0.54 (l)	91.2	0.67 (q)
s	c	r	u	s	79.0	0.61 (q)	76.0	0.79 (q)
s	c	r	u	r	81.0	0.57 (q)	78.8	0.73 (q)
s	c	r	c	s	94.3	0.57 (q)	91.2	0.71 (q)
s	c	r	c	r	95.1	0.56 (q)	92.6	0.68 (q)
r	u	s	u	s	56.9	0.66 (q)	54.2	1.01 (q)
r	u	s	u	r	61.3	0.65 (q)	54.4	1.00 (q)
r	u	s	c	s	67.8	0.62 (q)	65.0	0.76 (q)
r	u	s	c	r	71.2	0.59 (q)	64.6	0.78 (q)
r	u	r	u	s	57.7	0.66 (q)	52.0	0.89 (q)
r	u	r	u	r	59.3	0.65 (q)	52.2	0.94 (q)
r	u	r	c	s	70.6	0.61 (q)	63.5	0.81 (q)
r	u	r	c	r	70.9	0.61 (q)	62.7	0.80 (q)
r	c	s	u	s	81.3	0.75 (q)	80.2	1.25 (q)
r	c	s	u	r	84.3	0.67 (q)	81.4	1.24 (q)
r	c	s	c	s	96.0	0.67 (q)	95.6	0.91 (q)
r	c	s	c	r	96.9	0.62 (q)	95.9	0.90 (q)
r	c	r	u	s	78.6	0.67 (q)	77.1	1.02 (q)
r	c	r	u	r	80.2	0.67 (q)	78.3	1.02 (q)
r	c	r	c	s	96.6	0.62 (q)	95.6	0.93 (q)
r	c	r	c	r	96.8	0.62 (q)	95.7	0.91 (q)

s=smooth, specular reflections
r=rough, facets with slope of standard deviation = 1.0
c=clad with Lambertian reflector
u=unclad

for smooth sides to those for rough sides, it is clear that smooth sides are marginally better for the 3-mm thickness and significantly better for 6-mm thickness, despite there being less light collected than for rough sides. Quite clearly, treating the surface to increase the light output is not necessarily the best course to follow.

Another significant feature from these results is that cladding the surface opposite the photodetector array (bottom) improves the accuracy. This improvement is significantly more pronounced for the thicker crystal, and appears to be slightly more pronounced when the photodetector surface (top) itself is smooth. It is also noteworthy that the best result for the 6-mm-thick crystal, an average accuracy of 0.59 mm, is not significantly worse than that for the 3-mm-thick crystal of 0.52 mm, but more than 40% of the light must be sacrificed to achieve this result.

C. Positional Variability

In this section, we examine the dependence of the error in the 2-D POI on the location of the POI in the scintillator, for the 3-mm-thick case. In the previous section, we determined the average error in the 2-D POI for a large number of points generated at random throughout the entirety of the scintillator. In

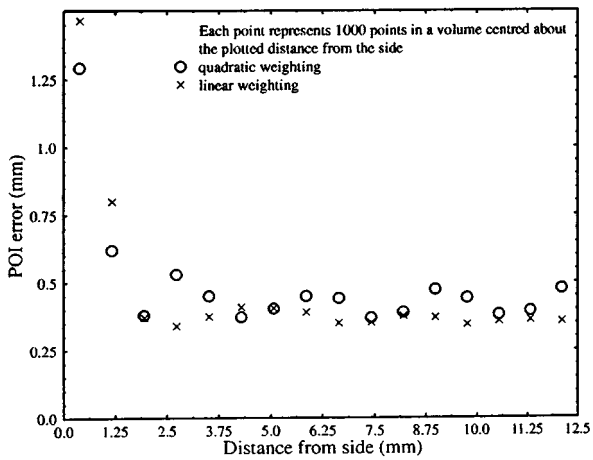

Fig. 2. Dependence of POI error on distance from side of crystal.

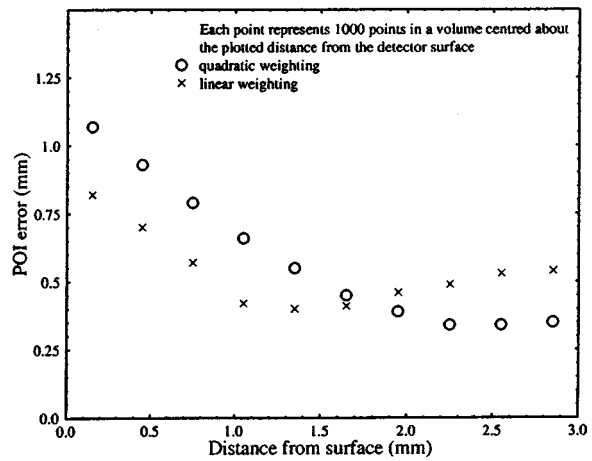

Fig. 3. Dependence of POI error on distance from photodetector surface.

practice, any application of this detector module is unlikely to result in gamma-ray interaction points with a uniform distribution . Here, we determine the average error for points randomly located within restricted volumes in the scintillator. There are two cases to consider. First, how does the error depend on distance from the edge, and secondly, how does the error depend on distance from the photodetector surface?

To examine the dependence of the 2-D POI error on the distance from the edge of the scintillator, we have used the code to generate 1000 interaction points at random, uniformly distributed throughout a restricted volume of the scintillator. The distance of the center of this volume from the edge of the crystal is then varied. This has been carried out for the surface conditions listed in the third row of Table II. The volume used was 3 mm high (the full thickness of the scintillator), 0.781 25 mm wide (one-quarter of the diode to diode spacing), and 3.125 mm long. The position of this volume was moved from one edge of the scintillator, directly under one of the central rows of diodes, toward the center of the scintillator. Fig. 2 below shows the results obtained. Clearly, the error throughout most of the crystal is much lower than for interaction points located near the edge. Thus, for applications where the gamma-rays are approaching from the edge of the module and hence are more likely to interact near the edge, it will be necessary to either develop a more sophisticated algorithm for the POI calculation, or modify the design of the module, if the average errors given in the previous section are to be achieved.

The second case to be examined is the dependence of the 2-D POI error on the distance from the photodetector surface. To look at this, we have considered volumes $25 \times 25 \times 0.3\ \text{mm}^3$ and used 1000 interaction points throughout this volume. The average error for the 1000 points has been determined for ten such volumes and is plotted in Fig. 3 below as a function of average distance from the photodetector surface. This has been done for two POI algorithms, using linear weighting of the four highest bin coordinates, and also using quadratic weighting.

Clearly, both algorithms give their worst results for points located near the photodetector plane, with the linear weighting giving a lower error here than the quadratic. Near the surface opposite the photodetector surface, the quadratic weighting gives the better result. Therefore, for applications where the gamma-rays would be entering through the surface opposite the photodetector surface, it would be better to use the quadratic weighting.

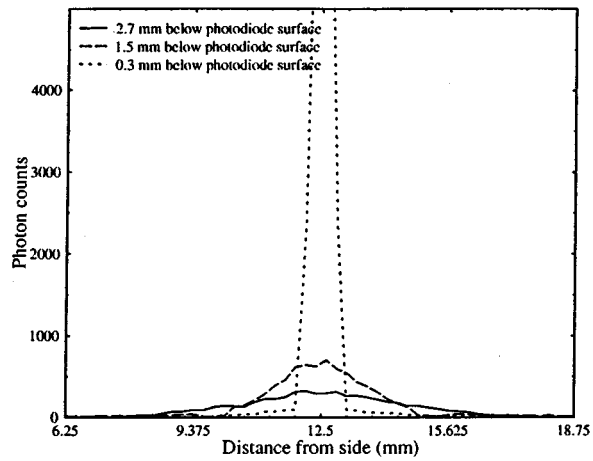

Fig. 4. Profiles through the light distribution for three different distances from the photodetector plane.

D. z Dependence of Light Distribution

Thus far, no mention has been made of extracting information about the z coordinate of the POI. This requires a more exacting analysis of the light distribution over the photodetector plane than is needed to extract the x–y information. In particular, what is needed is knowledge of how the light distribution varies as a function of distance from the photodetector plane and whether this variation may be reliably inferred from the 8×8 pixel map that we have of it.

In Fig. 4, we compare one-dimensional profiles, through the two-dimensional light distribution, for three different distances from the photodetector plane. These have been produced from 100×100 pixel maps and are for a scintillator 3 mm thick with all surfaces smooth and unclad. Remembering that for our 8×8 array the spacing between diode centers is 3.125 mm, it is clear that for the 3-mm-thick crystal we never get more than about two diodes' width for our light distribution.

The linear dependence of the full-width at half-maximum (FWHM) with distance from the photodetector is shown in

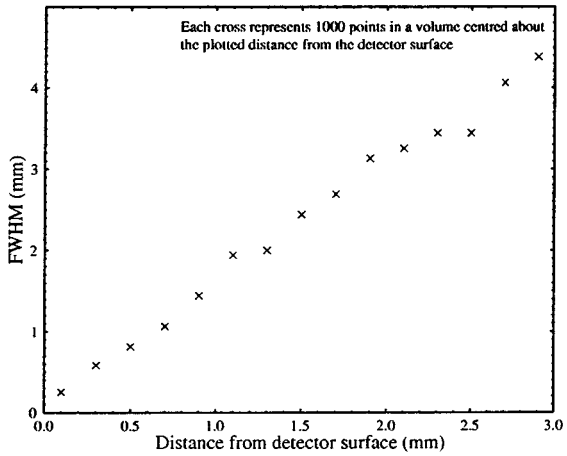

Fig. 5. Dependence of FWHM on distance from photodetector surface for points in middle of scintillator.

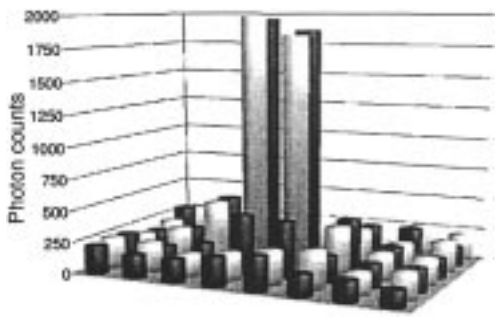

Fig. 6. Distribution of detected photons for interaction point in middle of scintillator and 2.7 mm from photodetector surface.

Fig. 5. This is for interaction points with x and y coordinates placing them in the middle of the crystal. The determination of the z coordinate of the point of interaction is thus reduced to determining the FWHM from the 8×8 pixel map of the light distribution. In Fig. 6, we show the distribution for an interaction point 2.7 mm from the photodetector surface and with x and y coordinates in the middle of the scintillator. This light distribution is not significantly different from that displayed in Fig. 1, despite there being a difference in the z coordinate of 1.2 mm. It appears then that extraction of the z coordinate from this light distribution will, if at all possible, be a considerable challenge.

E. Effect of Varying Signal-to-Noise Ratio (SNR)

For all the results reported so far in this paper, we have used 25 000 photons per gamma-ray interaction, assuming that any exit through the photodetector surface is detected, and used a noise figure of 200 electons rms in each diode. These figures were used, as we hope ultimately to be able to achieve close to this performance with our photodiode detectors when coupled to CsI(Tl) scintillators. However, to date it appears that our overall noise per diode, including electronics noise, is closer to 350 electrons rms. Therefore, it is useful to know how the accuracy of 2-D POI is affected by higher noise levels, and also by lower numbers of light photons. The simulations in Section III-B have been repeated with 350 electrons rms noise per photodiode, and both 20 000 and 10 000 photons per interaction. These values correspond to about the number of e–h pairs for CsI(Tl) and LSO scintillators, respectively [5]. Scintillator dimensions are $25 \times 25 \times 3$ mm^3. The results are given in Table III. The feature apparent from the results in this table is that the deterioration in 2-D POI accuracy when the signal decreases is only around 0.1 mm. When results from this table are compared to those from Table II, it can also be seen that with increased noise and reduced signal, the quadratic weighting algorithm always gives the best results. The difference between quadratic and linear weighting algorithm results is as high as 0.6 mm in 2-D POI accuracy for the signal and noise values used in Table III, whereas for the simulations in Table II the difference was marginal (on the order of 0.1 mm) in most cases.

TABLE III
DEPENDENCE OF 2-D POI ACCURACY ON SIGNAL WITH 350 E^- rms PER DIODE

Surface					20 000 photons		10 000 photons	
Sides		Bottom		Top	Output	Error	Output	Error
s	u	s	u	s	37.3	0.63 (q)	37.3	0.66 (q)
s	u	s	u	r	54.4	0.62 (q)	54.4	0.70 (q)
s	u	s	c	s	44.2	0.55 (q)	44.2	0.56 (q)
s	u	s	c	r	61.2	0.54 (q)	61.2	0.57 (q)
s	u	r	u	s	51.5	0.63 (q)	51.6	0.70 (q)
s	u	r	u	r	52.1	0.58 (q)	52.1	0.68 (q)
s	u	r	c	s	62.1	0.55 (q)	62.0	0.59 (q)
s	u	r	c	r	61.2	0.53 (q)	61.3	0.58 (q)
s	c	s	u	s	37.3	0.61 (q)	37.3	0.66 (q)
s	c	s	u	r	86.5	0.61 (q)	86.5	0.69 (q)
s	c	s	c	s	44.2	0.58 (q)	44.2	0.60 (q)
s	c	s	c	r	94.4	0.54 (q)	94.4	0.57 (q)
s	c	r	u	s	79.0	0.61 (q)	79.0	0.70 (q)
s	c	r	u	r	81.0	0.61 (q)	81.0	0.70 (q)
s	c	r	c	s	94.3	0.55 (q)	94.4	0.57 (q)
s	c	r	c	r	95.1	0.55 (q)	95.1	0.71 (q)
r	u	s	u	s	56.9	0.66 (q)	57.0	0.79 (q)
r	u	s	u	r	61.2	0.67 (q)	61.2	0.78 (q)
r	u	s	c	s	67.8	0.62 (q)	67.7	0.67 (q)
r	u	s	c	r	71.2	0.60 (q)	61.2	0.68 (q)
r	u	r	u	s	57.7	0.66 (q)	57.7	0.78 (q)
r	u	r	u	r	59.3	0.65 (q)	59.3	0.77 (q)
r	u	r	c	s	70.5	0.63 (q)	70.6	0.70 (q)
r	u	r	c	r	70.9	0.61 (q)	70.9	0.67 (q)
r	c	s	u	s	81.3	0.79 (q)	80.2	1.00 (q)
r	c	s	u	r	84.3	0.71 (q)	84.3	0.84 (q)
r	c	s	c	s	96.0	0.69 (q)	96.0	0.91 (q)
r	c	s	c	r	96.9	0.67 (q)	95.9	0.75 (q)
r	c	r	u	s	78.6	0.69 (q)	78.7	0.82 (q)
r	c	r	u	r	80.2	0.69 (q)	80.3	0.81 (q)
r	c	r	c	s	96.6	0.64 (q)	96.6	0.74 (q)
r	c	r	c	r	96.8	0.63 (q)	96.7	0.74 (q)

s=smooth, specular reflections
r=rough, facets with slope of standard deviation = 1.0
c=clad with Lambertian reflector
u=unclad

IV. CONCLUSION

We have shown that with our design of a gamma-ray detector module, it should be possible to measure the 2-D POI to around 0.6 mm accuracy. This result can be obtained with signal levels varying from 25 000 photons to 10 000 photons, and with noise per diode of 200 to 350 e^- rms. This figure of 0.6 mm could be reduced by improving the accuracy of this calculation for interactions occurring near the sides of the scintillator and near

the detector surface. Further work also needs to be done on methods of reliably estimating the third coordinate of the interaction point. At present, knowldege of this third coordinate is limited to the thickness of the scintillator, that is, 3 mm. If interaction points are distributed uniformly with z , and we assume the value of z to be always in the middle of the crystal, then this will lead to an overall average error in the 3-D POI of around 1 mm.

ACKNOWLEDGMENT

The authors would like to acknowledge the contributions of G. Taylor and S. Lindsay of the University of Melbourne for discussions in the early stages of this work, particularly for providing details of similar simulations carried out for BGO crystals; V. Perevertailo, of SPA "Detector," Kiev, who assisted in the design of the diodes and oversaw their manufacture; and S. Meikle and S. Eberl of Royal Prince Alfred Hospital, Sydney, for contributing their ideas on applications of the detector modules under development.

REFERENCES

[1] B. E. Patt, J. S. Iwanczyk, C. R. Tull, N. W. Wang, M. P. Tornai, and E. J. Hoffman, "High resolution CsI(Tl)/Si-PIN detector development for breast imaging," *IEEE Trans. Nucl. Sci.*, vol. 45, pp. 2126–2131, Aug. 1998.

[2] W. W. Moses and S. E. Derenzo, "Design studies for a pet detector module using a PIN photodiode to measure depth of interaction," *IEEE Trans. Nucl. Sci.*, vol. 41, pp. 1441–1445, Aug. 1994.

[3] S. Yin, T. O. Tumer, D. Maeding, J. Mainprize, G. Mawdsley, M. J. Yaffe, and W. Hamilton, "Hybrid direct conversion detectors for digital mammography," *IEEE Trans. Nucl. Sci.*, vol. 46, pp. 2093–2097, Dec. 1999.

[4] O. Toker, S. Masciocchi, E. Nygard, A. Rudge, and P. Weilhammer, "VIKING, a CMOS low noise monolithic 128 channel frontend for Si-strip detector readout," *Nucl. Instrum. Meth. Phys. Res. A*, vol. 340, pp. 572–579, 1994.

[5] M. Moszynski, M. Kapusta, M. Mayhugh, D. Wolski, and S. O. Flyckt, "Absolute light output of scintillators," *IEEE Trans. Nucl. Sci.*, vol. 44, pp. 1052–1061, June 1997.

[6] S. Siegel, S. R. Cherry, A. R. Ricci, Y. Shao, and M. E. Phelps, "Development of continuous detectors for a high resolution animal PET system," *IEEE Trans. Nucl. Sci.*, vol. 42, pp. 1069–1074, Aug. 1995.

[7] G. F. Knoll, T. F. Knoll, and T. M. Henderson, "Light collection in scintillation detector composites for neutron detection," *IEEE Trans. Nucl. Sci.*, vol. 35, pp. 872–875, February 1988.

[8] M. L. F. Lerch, A. B. Rosenfeld, P. E. Simmonds, G. Taylor, S. Meikle, and V. Perevertailo, "Spectral characterization of a blue enhanced silicon photodector," in *IEEE NSS/MIC 2000 Conf. Rec.*, submitted for publication.

[9] S. E. Holland, N. W. Wang, and W. W. Moses, "Development of low noise, back-side illuminated silicon photodiode arrays," *IEEE Trans. Nucl. Sci.*, vol. 44, pp. 443–447, June 1997.

[10] J. Bea, A. Gadea, L. M. Garcia, J. Rico, B. Rubio, and J. L. Tain, "Simulation of light collection in scintillators with rough surfaces," *Nucl. Instrum. Meth. Phys. Res. A*, vol. 350, pp. 184–191, 1994.

[11] A. Levin and C. Moisan, "A more physical approach to model the surface treatment of scintillation counters and its implementation into DETECT," in *1996 IEEE Nuclear Science Symp. Conf. Rec. 2*, 1997, pp. 702–706.